Supramolecular Self-Assembly of Glutamine Synthetase: Mutagenesis of a Novel Intermolecular Metal Binding Site Required for Dodecamer Stacking†

Michael J. Dabrowski,‡ Joseph Yanchunas, Jr.,§ Beth Cader Villafranca,|| Eric C. Dietze,‡ Peter Schurke,‡ and William M. Atkins*,‡

Department of Medicinal Chemistry, School of Pharmacy, BG-20, University of Washington, Seattle, Washington 98195, Macromolecular Structure Division, Bristol-Myers Squibb, Box 4000, Princeton, New Jersey 08543-4000, and Department of Chemistry, Frick Laboratory, Princeton, New Jersey 08544

Received July 15, 1994; Revised Manuscript Received September 19, 1994®

ABSTRACT: Dodecameric glutamine synthetase (GS) from *Escherichia coli* assembles into highly ordered supramolecular protein tubes in the presence of several divalent metal ions. The molecular mechanism for this metal-induced self-assembly of the *E. coli* GS has been studied by molecular modeling and site-directed mutagenesis. The X-ray crystal structure of the nearly identical *Salmonella typhimurium* GS has been used to construct a model of the "stacked" complex between two dodecamers. A complementary fit, based on steric constraints, reveals a possible interaction between the N-terminal helices from adjacent dodecamers. The amino acid side chains of His and Met residues within the helices from each of the subunits of one face of a dodecamer lie within ~3.5 Å of the analogous side chains in the subunits from the adjacent dodecamer in the stacked complex. His-4, Met-8, and His-12 from adjacent helices provide potential ligands for a binuclear metal binding site. Replacement of each of these surface residues with aliphatic amino acids has negligible effects on the enzymatic activity, the regulation of activity via adenylylation, and gross dodecameric structure. However, the rate and extent of metal ion-mediated self-assembly of GS tubules are reduced to <2% of the wild-type protein in the single mutants H4A, H12L, and H12D. The M8L mutant demonstrates a 3-fold decrease in the bimolecular rate constant for stacking, but electron microscopy indicates that this mutant does form stacked tubes. The cysteine-containing mutants H4C, M8C, and H12C were also constructed. The stacking ability is partially recovered in the H12C and H4C mutant proteins, and the M8C protein stacks with an apparent bimolecular rate constant that is 8-fold faster and 2-fold faster than that of the wild-type protein with Zn^{2+} and Co^{2+}, respectively. In contrast, the M8C mutant does not stack with Cu^{2+}. The interface between dodecamers within the complex is dominated by polar residues, and the proposed model indicates that the interface remains partially solvated. These results indicate that the mechanism of self-assembly of *E. coli* GS to form stacked tubules involves an interdodecameric metal binding site formed from histidine residues at the i and $i + 8$ positions of two adjacent helices and a methionine at $i + 4$.

De novo design of proteins which possess useful supramolecular architecture may eventually provide novel materials with applications in biomaterials (Stayton et al., 1992), biomineralization (Meldrum et al., 1991), and other nanotechnologies. Metal ion-assisted peptide folding and aggregation provide one tool for *de novo* design of protein-based materials and catalysts (Ghadiri et al., 1992). Metal binding sites have been shown to initiate the formation of secondary structure in synthetic peptides, and they have stabilized "native-like" tertiary structure in molten globule proteins [see Berg (1993) and Betz et al. (1993) for reviews]. Furthermore, metal ions have been exploited to obtain aggregates of peptides and peptide/DNA complexes (Berg, 1993). It also would be useful if engineered metal binding sites could be used to direct assembly of macromolecular protein aggregates of defined quaternary structure. At this early stage of protein engineering, it is essential to identify novel, naturally occurring, metal binding sites which may be used for these purposes. Here we present a model for an intermolecular binuclear metal site which directs the supramolecular assembly of protein tubules from *Escherichia coli* glutamine synthetase (GS).[1] In addition, the metal specificity of the site for Zn^{2+} vs Cu^{2+} has been reversed by site-directed mutagenesis.

Bacterial glutamine synthetases (GS) are dodecameric aggregates formed from several types of subunit interactions. The individual dodecamers are formed from two face-to-face hexameric rings of identical subunits. In addition, some dodecameric GS isozymes "stack" face to face to form tubules in the presence of Cu^{2+}, Zn^{2+}, Hg^{2+}, Co^{2+}, and other divalent metal ions. The physiological role of this reaction has not been established. In the accompanying papers we have characterized the solution conditions which affect the

† This work was supported by the National Science Foundation (MCB-9305202) and by the Whitaker Foundation (93-0272).

* Corresponding author [telephone (206) 685-0379; FAX (206) 685-3252].

‡ University of Washington.

§ Bristol-Myers Squibb.

|| Frick Laboratory.

® Abstract published in *Advance ACS Abstracts,* November 1, 1994.

[1] Abbreviations: GS, glutamine synthetase; PCR, polymerase chain reaction; keV, kiloelectronvolts; EM, electron microscopy. Mutant proteins are identified by the standard system in which the single-letter amino acid abbreviation of the wild-type residue is followed by the amino acid number and the single-letter abbreviation for the amino acid substituted; e.g., H4A is the mutant in which histidine-4 is replaced with an alanine.

0006-2960/94/0433-14957$04.50/0

kinetics of this reaction (Yanchunas et al., 1994), and we have determined the kinetic parameters $\Delta H^{\ddagger}$ and $\Delta V^{\ddagger}$ for formation of the encounter complex en route to the "stacked" dodecameric assembly (Atkins, 1994). These parameters provide useful insights into the protein−solvent and protein−protein interactions involved in GS stacking, but the mechanism for this macromolecular recognition remains unknown. Although this self-assembly process was discovered 2 decades ago (Miller et al., 1974), few data have addressed directly the mechanism of this reaction.

On the basis of previous studies of the metal-dependent formation of stacked GS complexes, it has been suggested that the metal ions bind to individual dodecamers and induce a conformational change which allows the protein to self-assemble into tubules (Miller et al., 1974). Here we present evidence for a metal binding site formed at the interface of stacked GS dodecamers, and we propose that "bridging" metal ions stabilize the stacked complex, without a significant conformational change of the individual dodecamers. Identification of the metal ligands is the essential first step toward manipulation of the metal specificity of this reaction. An understanding of this metal binding site may provide control of production of protein tubles from GS.

MATERIALS AND METHODS

Assay for GS Stacking. The stacking reaction of wild-type and mutant GS proteins was monitored by 90° light scattering measurements and electron microscopy, as described in the accompanying papers (Yanchunas et al., 1994; Atkins, 1994). Samples contained 0.17 μM GS subunits in 50 mM Hepes, pH 7.0, 100 mM KCl, and 1 mM $MnCl_2$ at 5 °C. Light scattering data obtained after addition of metal ion were used to calculate second-order rate constants or reaction half-times, as described previously (Yanchunas et al., 1994). Conditions for individual experiments are given in the table legends.

Site-Directed Mutagenesis. Site-directed mutants were constructed by two methods. The "megaprimer" method (Sarkar & Sommer, 1990) was used for construction of the H4A, M8L, M8C, and H12D mutants. All PCR experiments utilized the following initial conditions: 10 mM KCl, 10 mM $(NH_4)_2SO_4$, 20 mM Tris-HCl (pH 8.3), 3 mM $MgSO_4$, 200 μM each dNTP, 0.1% Triton X-100, 10 ng of linearized PCR plasmid template pTZglnA, and 100 pmol of oligonucleotide primers in 100 μL. The oligonucleotides used to generate the megaprimer spanned the *Bsu*36I restriction site, which lies 300 nucleotides outside the 5′-end of the GS gene, and the site of mutation (Colombo & Villafranca, 1986). The cycle profile for amplification of the mutant megaprimer was 1 min at 94 °C, 1 min at 65 °C, and 2 min at 72 °C, for 25 cycles, followed by a single 10-min extension at 72 °C. The amplified fragment was used in a second round of PCR with an oligonucleotide spanning the *Bgl*I restriction site which is contained in the GS gene (Colombo & Villafranca, 1986). The final mutant-encoding fragment was digested with *Bsu36I* and *Bgl*II and then ligated into the plasmid pgln35 for expression of mutant protein. The H12L, H12C, and H4C mutant proteins were constructed by the overlap extension method (Ho et al., 1989), using the same conditions as above to generate subfragments with overlap at the site of mutation and spanning either the *Bsu*36I site or the *Bgl*II site. These subfragments were used to generate the full-length, mutant fragment, subsequently cloned into the plasmid pgln35 using these restriction sites.

Protein Purification. Wild-type GS and the M8C and H12C mutant proteins were purified as described in the accompanying paper (Yanchunas et al., 1994). Purification of the H4A, H4C, M8L, H12D, and H12L mutant proteins required modification of this procedure. Because these proteins do not precipitate quantitatively upon addition of Zn^{2+}, this step was not included in the purification protocol. Instead, the supernatant resulting from the streptomycin sulfate precipitation was dialyzed exhaustively against 20 mM Hepes, pH 7.0, 100 mM KCl, and 1 mM $MnCl_2$, and the acetone precipitation and ammonium sulfate precipitation steps were performed as with the wild-type protein (Yanchunas et al., 1994). The final pool of GS was then purified by Affi-Gel Blue (Bio-Rad) column chromatography, in 20 mM Hepes, pH 7.0, 1 mM $MnCl_2$, and 100 mM KCl, using 20 mM ADP in the same buffer to elute the mutant proteins. ADP was removed from the pooled fractions containing GS by gel filtration. The mutant proteins purified by this procedure were >95% homogeneous, based on overloaded SDS−PAGE gels.

Molecular Modeling. Molecular modeling was performed with the software package MidasPlus (UCSF) on a Silicon Graphics Indigo workstation, using the X-ray crystal structure of the substrate-free *Salmonella typhimurium* GS (Yamashita et al., 1990). Solvent-accessible surfaces were calculated using default parameters (probe radius 1.4 Å).

Electron Microsopy. Transmission electron micrographs were obtained on a JEOL microscope, 80 keV, at 60000× magnification. Samples were prepared by placing a drop of purified wild-type or mutant GS on a Formvar-coated copper grid (200 mesh) for 2 min. The grid was blotted dry and negatively stained with 2% uranyl acetate for 4 min. The grid was blotted dry and air-dried. Samples were prepared immediately prior to microscopy.

RESULTS

Model of the Stacked Complex. Dodecameric GS enzymes consist of 12 identical subunits arranged as two face-to-face hexameric rings. A 6-fold axis of symmetry runs through the center, normal to the plane of the double-layered hexagon (Figure 1A; Almassy et al., 1986; Yamashita et al., 1991). The crystal structure of the substrate-free *S. typhimurium* GS was used as a model for possible protein−protein interactions between adjacent *E. coli* dodecamers in a stacked complex. The *E. coli* and *S. typhimurium* enzymes exhibit 98% identity in amino acid sequence. The *S. typhimurium* GS also forms specific, ordered tubes in the presence of some metal ions. An initial model for the stacked complex of two dodecameric GS molecules was obtained by considering the previously reported results from electron microscopy and optical image analysis of the Co^{2+}-precipitated complex of *E. coli* GS (Frey et al., 1975). These electron micrographs indicate that two adjacent dodecamers in a stacked complex are rotated approximately 8° relative to one another about the 6-fold axis of symmetry. When molecular models of two dodecamers are brought together in a face-to-face orientation, it is apparent that a complementary steric fit is possible (Figure 1A). Specifically, each subunit within a dodecamer contains, at its N-terminus, a 15-residue α-helix which lies down on the face of the ring structure, leaving the helical axes nearly

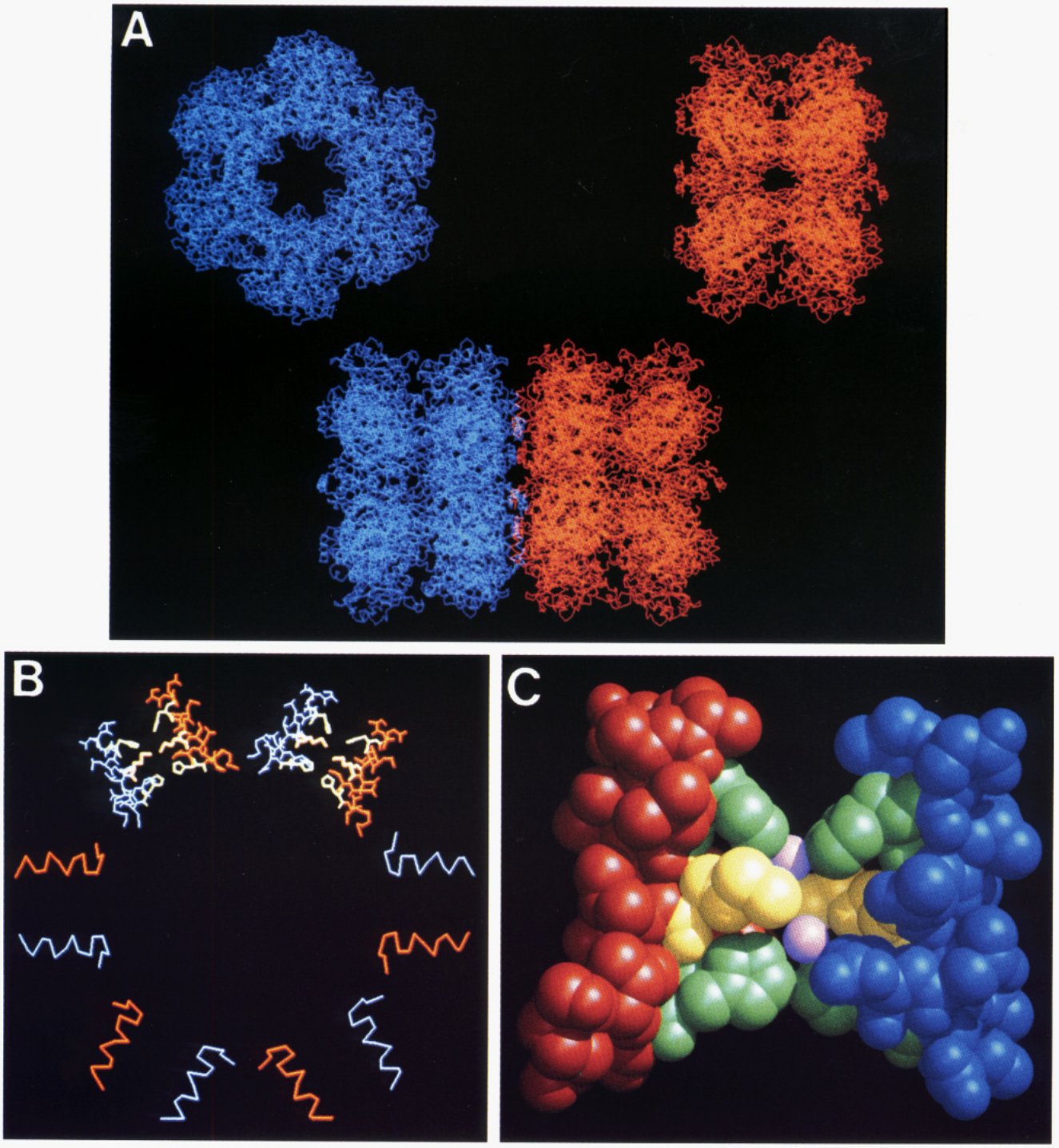

FIGURE 1: Molecular model for the docked complex of GS dodecamers. (A) The α-carbon trace of one dodecamer is shown with the 6-fold axis of symmetry perpendicular to the page (top left, blue), and a second dodecamer is shown with the 6-fold axis running horizontally within the plane of the page (top right, red). A docked complex of the two dodecamers is shown, with the 6-fold axis horizontally within the page. (B) The α-carbon trace of the N-terminal helices (residues 1−15) of six subunits from one dodecamer (red) and six subunits of a second dodecamer (blue) at the interdodecameric interface is shown. This figure is obtained from the docked complex shown in (A). All residues not contained in the N-terminal helices have been removed, and the complex is rotated so the 6-fold axis runs perpendicular to the page. For two pairs of N-terminal helices, amino acid side chains have been included. His-4 (green) is closest to the outer perimeter, His-12 (green) is closest to the center, and Met-8 (yellow) lies between them. (C) The space-filling model of one helix−helix interaction is shown. One Zn^{2+} (pink) has been placed between His-4 (top, green) and Met-8 (yellow), and a second lies between His-12 (bottom, green) and Met-8. The rotamer conformations of the side chains have not been changed from the X-ray structure, although side-chain rotation is required to optimize the metal binding sites (Table 1).

perpendicular to the 6-fold axis of symmetry that runs through the dodecamer. The individual helices from the six subunits on one flat face of the dodecamer collectively form the "spokes of a wheel" emanating from the 6-fold axis. When one dodecamer is juxtaposed near a second molecule and rotated 10° relative to the 6-fold axis, the "spokes" of one dodecamer lie between the spokes of the second. The spokes form ridges on each dodecameric face, with valleys between each pair of helices. Thus, the ridges formed from the N-terminal helices of one dodecamer lie in the valleys between the ridges on the docked dodecamer (Figure 1B). Furthermore, maximal steric complementarity is achieved

Table 1: Interatomic Distances for Metal Ions and Protein Ligands in the Proposed Metal Binding Site[a]

atoms	minimum distance after side-chain rotation (Å)
His-12 δN···metal 1	3.68
His-12 ϵN···metal 1	2.47
Met-8 δS···metal 1	3.46
Met-8 δS···metal 2	3.03
His-4 δN···metal 2	4.63
His-4 ϵN···metal 2	3.43

[a] The reported distances are the average of the distances from the metal ion to the specified atom in each of the two helices. For metal 1, either δN or ϵN atoms of His-12 are ligands, and similarly either δN or ϵN atoms of His-4 are ligands for metal 2. Distances are based on the radius of Zn^{2+} found in carboxypeptidase.

when one dodecamer is rotated approximately 8−9° about the 6-fold axis of symmetry, relative to the second dodecamer, in close agreement with the relative orientation observed by Frey et al. (1975). Examination of the helices on adjacent dodecamers indicates that two histidines and a methionine are contained in each of the N-termini. The side chains of His-4 and His-12 are directed toward the analogous side chains in the helix from the adjacent subunit. The Met-8 side chains lie above and below the histidines, and they form "caps" covering the space between these adjacent helices. This arrangement of His and Met side chains provides six potential metal-coordinating ligands which are ideally oriented to ligate divalent metal ions (Figure 1C). The model depicted in Figure 1C includes two metal ions for reasons which are outlined in the Discussion. The precedent for histidine ligation of Zn^{2+}, Cu^{2+}, and Co^{2+} in proteins is extensive (Karlin, 1993; Glusker, 1991). Methionines are less frequently found at metal binding sites, although several examples are known (Rosenfield, 1977; Chakrabarti, 1989). In the model shown in Figure 1, the rotamer conformations of the amino acid side chains are exactly as found in the X-ray structure. Obviously, rotation of these side chains is required for optimal geometry of metal ligands. In particular, the side chains of Met-8 would be expected to rotate so that the δS atom is oriented toward the metal ions, and the His side chains may rotate so that either the δN or the ϵN atoms provide metal ligands. The distances between metal ions and relevant atoms in His-4, His-12, and Met-8 after optimization via rotation of side chains are summarized in Table 1. Based on these distances, it is not possible to determine whether ϵN atoms or δN atoms of His-12 and His-4 provide ligands to the metal ions. The metal ions were positioned to afford minimum distance to one pair of histidines (His-4 or His-12) and one of the Met-8 sulfur atoms. The distances associated with the metal near His-4 (arbitrarily labeled metal 2) are at the upper limit of distances found in other naturally occurring metal sites in proteins. It is possible that additional rearrangement of the dodecamers and of the individual side chains may decrease these distances. Due to the size of GS (7200 atoms × 12 subunits excluding solvent), we have not attempted free energy minimization or molecular dynamics simulations with the docked complex. Therefore, this model provides a working hypothesis for the molecular mechanism of metal-induced GS stacking, but it is not refined sufficiently to predict the actual location of amino acid side chains and of the metal ions.

Additional support for this molecular model is obtained from consideration of the amino acid sequences of bacterial GS isozymes (Wray et al, 1988; Pesole et al., 1991). All GS dodecamers which have been reported to precipitate in the presence of Zn^{2+} possess these histidines and the methionine, whereas these residues are all absent in the GS dodecamers which do not stack in the presence of metal ions. Furthermore, biochemical evidence suggests that exposed histidines are critical for Zn^{2+}-induced stacking of GS. Modification of two histidines/subunit abolishes GS stacking (Yanchunas et al., 1994). As a result of this sequence comparison, the preliminary molecular model, and these chemical modification experiments, His-4, Met-8, and His-12 became candidates for site-directed mutagenesis, in order to determine whether these residues play a role in the metal-dependent self-assembly of GS tubes.

Characterization of Mutant Proteins. The enzymatic activities and regulatory properties of each of the site-directed mutants H4A, H12L, H12D, and M8L were examined and compared to the wild-type protein, in order to determine whether the mutations induced significant structural changes. The activities of each of these proteins were determined by the γ-glutamyl transferase assay (Woolfolk et al., 1966). In addition, the sensitivity to adenylylation was determined for each mutant (Ginsburg et al., 1970). *E. coli* GS is regulated *in vivo* by covalent adenylylation of Tyr-397. This covalent modification alters the metal ion specificity for the metals which are bound at the active site. The unadenylylated enzyme is active with both Mn^{2+} and Mg^{2+} bound at the active site. These metal binding sites are distinct from the interdodecameric metal binding sites proposed above. Adenylylation of the Mg^{2+}-bound wild-type enzyme results in inactivation. The differential activity in the presence of Mn^{2+} vs Mg^{2+} provides a quantitative measure of the adenylylation state of the enzyme. Also, comparison of the catalytic properties of the adenylylated and the unadenylylated mutant proteins provides a sensitive probe of the active site structure. These activity assays indicate that each of these mutant proteins has steady-state catalytic and regulatory properties that are nearly identical to those of the wild-type enzyme. Moreover, this characterization of the mutant proteins was necessary to ensure that each was fully unadenylylated. It is demonstrated in the accompanying paper (Atkins, 1994) that adenylylation of wild-type GS results in a decreasee in the rate of Zn^{2+}-induced stacking. Therefore, it was necessary to demonstrate that the adenylylation states of each mutant and wild-type GS were identical. These results are summarized in Table 2.

Each of the mutant proteins also was examined by electron microscopy (EM), as described in the accompanying paper (Yanchunas et al., 1994). EM provides a probe of gross dodecameric structure [see Yanchunas et al. (1994) for examples]. It is clear from electron micrographs that each of these mutant proteins maintains an intact dodecameric ring structure that, presumably, is required for the metal-dependent self-assembly reaction (data not shown). Apparently, these mutations at positions 4, 8, and 12 do not prevent the Chaperonin-assisted assembly of dodecameric GS (Fisher, 1990).

Having established that the mutant proteins retain the dodecameric ring structure and that each is fully unadenylylated, light scattering experiments were performed in order to determine the effect of these mutations on the metal-

Table 2: Catalytic Activity of Mutant Proteins

protein[a]	transferase activity, Mn^{2+} (units/mg)[b]	adenylylation state, transferase assay[c]
wild type, $n = 0$	132 ± 9	0.2 ± 0.1
wild type, $n = 12$	136 ± 9	12.4 ± 0.9
H4A, $n = 0$	129 ± 3	0.3 ± 0.4
H4A, $n = 12$	136 ± 7	12.0 ± 0.7
M8L, $n = 0$	115 ± 1	0.4 ± 0.7
M8L, $n = 12$	119 ± 9	11.9 ± 0.5
H12L, $n = 0$	139 ± 8	0.8 ± 0.6
H12L, $n = 12$	ND[d]	ND
H12D, $n = 0$	136 ± 5	0.6 ± 0.8
H12D, $n = 12$	130 ± 6	11.7 ± 0.6
H4C, $n = 0$	31 ± 3	0.8 ± 0.5
M8C, $n = 0$	125 ± 7	0.3 ± 0.8
H12C, $n = 0$	117 ± 7	0.7 ± 0.4

[a] $n = 0$ refers to fully unadenylylated GS; $n = 12$ refers to fully adenylylated GS. The preparations are referred to as either $n = 0$ or $n = 12$ because they are isolated from bacterial strains which only produce one form. The experimentally determined values of the adenylylation state are included in the right-hand column. [b] Transferase assay according to Woolfolk et al. (1966). [c] Adenylylation assay according to Stadtman et al. (1979). [d] ND, not determined.

induced stacking reaction. For each mutant, and for wild-type GS, light scattering experiments were performed as described in Materials and Methods and as demonstrated in the accompanying papers. Results for the Zn^{2+}-mediated reaction are shown in Figure 2. The M8L mutant exhibits a 2-fold reduction in apparent second-order rate constant, but this protein efficiently forms stacked complexes. In contrast, the H4A, H12L, and H12D mutant proteins all exhibit a dramatic reduction in their ability to form tubules in the presence of Zn^{2+} (Table 3). The results were confirmed by EM experiments; no stacking is evident for the H4L, H12L, or H12D mutants (Figure 2). It is noteworthy that the H12D mutant does not stack. Because many Zn^{2+}-containing proteins possess carboxylate metal ligands, we believed it possible that this mutant would exhibit metal-dependent stacking.

In addition to the Zn^{2+}-initiated self-assembly of GS tubules, the abilities of these mutant proteins to stack in the presence of other metal ions were examined. Essentially identical results were obtained with Cu^{2+}, and Co^{2+}, as observed for the Zn^{2+} reaction (Table 3). The H4D and H4L mutant proteins do not stack in the presence of these other metal ions. As with Zn^{2+}, the M8L mutant protein does form stacked complexes, but at a significantly reduced rate. The concentration dependences of the stacking reactions initiated by Zn^{2+}, Cu^{2+}, and Co^{2+} for the mutant proteins also were examined. For each mutant, the bimolecular rate constants for stacking were determined at six concentrations of each metal ranging from 10 μM to 10 mM. At each metal concentration, the relative difference between the rate of stacking for each mutant compared to that of the wild type was nearly identical to the values reported in Table 3. The concentrations of metal ions shown in Table 3 afford nearly identical rates of stacking of the wild-type protein (Yanchunas et al., 1994). Thus, the differences between the mutant proteins and the wild type are maintained over a wide metal ion concentration range. Taken together, these results suggest that the heteroatoms of the side chains at positions 4 and 12 are essential for ligation of all of the metal ions which induce GS stacking.

Because cysteine side chains have been found to substitute for histidine ligands in many Zn^{2+} binding proteins and Cu^{2+}

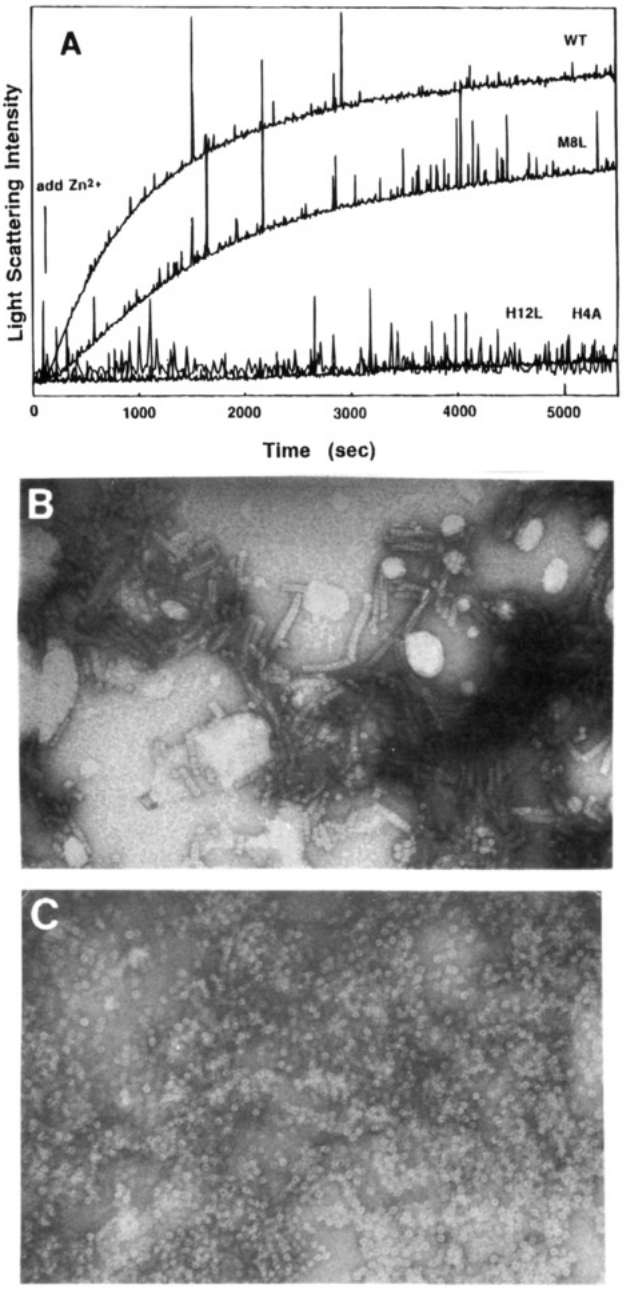

FIGURE 2: Zn^{2+}-induced stacking of wild-type and mutant GS. (A) The intensity of scattered light was monitored following addition of Zn^{2+}. Electron micrographs of samples containing wild-type GS (B) or H4A (C) 3000 s after addition of 100 μM $ZnCl_2$ are shown. The H4A and H12L mutants stack with dramatically reduced bimolecular rate constants.

binding proteins, the H4C, M8C, and H12C mutants were also constructed, and they were analyzed for their ability to form tubules in the presence of Zn^{2+}, Cu^{2+}, and Co^{2+}. These mutant proteins were also characterized by the γ-glutamyl transferase assay, and the catalytic activities are included in Table 2. The H4C and H12C mutant proteins demonstrate a bimolecular rate constant for stacking that is reduced compared to that for the wild-type protein, but it is clear that these cysteine side chains support metal binding and GS stacking (Table 3). Interestingly, the H4C mutant does not form tubules in the presence of Zn^{2+} as readily as the H12C mutant. This is consistent with the minimum distances between the histidine heteroatoms and the metal ions reported in Table 1. Because the axes of the N-terminal helices

Table 3: Relative Rates of Metal-Induced Stacking for Wild-Type and GS Mutants

protein	relative bimolecular rate constant[a]		
	Zn^{2+} (100 μM)	Cu^{2+} (10 μM)	Co^{2+} (1 mM)
WT	1.00	1.00	1.00
H4A	0.080	0.030	<0.002
H12L	0.048	0.034	<0.21
H12D	0.007	0.019	ND[b]
M8L	0.385	0.167	0.690
H4C	0.240	0.120	0.040
H12C	0.452	0.257	2.15
M8C	8.57	0.244	1.471

[a] Rates for each mutant are relative to wild type for the same metal ion. For comparison of relative rates for varying metals, see Figure 5 in Yanchunas et al. (1994). Reaction rates were measured at the following concentrations of each ion: Zn^{2+}, 100 μM; Cu^{2+}, 10 μM; Co^{2+}, 1 mM. These concentrations of metal ions give approximately equivalent rates of stacking for wild-type GS. Reactions contained 0.17 μM GS (dodecamers) in 50 mM Hepes, pH 7.0, 100 mM KCl, and 1 mM $MnCl_2$ at 5 °C. [b] ND, not determined.

diverge toward the outer perimeter of the ring structure, the His-4 side chains are further apart than the side chains of the His-12. Therefore, replacement of His-4 with the shorter cysteine side chain may provide a good metal ligand which is poorly situated for metal ligation.

An additional striking result is that the M8C mutant protein stacks significantly faster than the wild type for the Zn^{2+}- and Co^{2+}-mediated reactions. Also, the H12C reacts significantly faster than the wild type in the Co^{2+}-initiated assembly of tubules. The fact that the cysteine side chains can provide "better" metal ligands than the wild-type histidines strongly implicates the side chains of residues 4 and 12 as metal ligands in the stacking reaction. Additional experiments are required to explain in structural terms the differential metal ion specificities of these mutants.

The Dodecamer–Dodecamer Interface. Having demonstrated that His-4, Met-8, and His-12 contribute to an intermolecular metal binding site, the interface between dodecamers was examined for other molecular interactions. It is apparent that the majority of amino acid residues at the dodecamer interface are charged or polar. Only 30–35% of the side chains at the GS stacking face are hydrophobic. The van der Waals surface of the dodecamer–dodecamer interface is shown in Figure 3. It is striking that large gaps are present between the dodecamers, when the geometry of metal binding site is optimized for ligation to tetrahedral or octahedral coordination to metal ions. That is, the interface between the dodecamers is not close packed and desolvated. Rather, there are solvent pockets between the individual subunits contained in different dodecamers. These solvent pockets are easily accommodated by the polar interface. When a close-packed interface is formed by "forcing" the two dodecamers together, the metal binding site is destroyed. Thus, stacked GS represents a tightly bound protein complex (K_d < 3 nM; Atkins, 1994) that does not have extensive van der Waals contact between the bound proteins. The solvent-accessible surface has been calculated for a subset of the stacking interface, specifically the face of a single subunit on the surface facing an adjacent dodecamer. The solvent-accessible surface area of the stacking face of a single subunit is ~3000 Å^2, but examination of the surface of two subunits in a stacked complex indicates that only a small fraction of this surface is buried upon complex formation. In fact, only the portions of the N-terminal helices which provide metal binding sites would be expected to undergo significant desolvation when one dodecamer is stacked onto a second GS molecule (Figure 3).

DISCUSSION

The molecular mechanism of tubule formation from GS dodecamers has been studied by molecular modeling and site-directed mutagenesis. In the model proposed here, two metal binding sites are formed between the N-terminal helices of adjacent subunits in stacked dodecamers. This corresponds to a total of 12 metal binding sites at each dodecamer interface. His-4, Met-8, and His-12 from two of these helices provide potential metal-ligating side chains. When this model was constructed, we assumed that either the [(His-4)-(Met-8)]$_2$ or the [(His-12)-(Met-8)]$_2$ combination of amino acids would provide a single tetravalent metal site between the N-terminal helices. The fact that the H4A and H12L single mutants do not stack in the presence of metal ions suggests that both His-4 and His-12 are required for dodecamer–dodecamer stacking. This raises the possibility that the intermolecular metal binding site is binuclear, because the distance between the heteroatoms of His-4 and His-12 is too far apart (~8 Å) to provide ligands to a single metal ion. In order to account for the fact that metal ligands are required at both position 4 and position 12, we must consider the possibility that the metal binding site accommodates two ions. When one metal ion is placed between His-4 and Met-8 and a second is placed between Met-8 and His-12, this affords two trivalent sites, with one Met-8 providing a ligand to one of the metal ions and the Met-8 from the other helix providing a ligand to the other ion. This would require that water molecules provide the remaining ligands, as observed with "catalytic Zn^{2+} sites" (Glusker, 1991). On the basis of the solvent accessibility of the interface, water molecules are readily available. A striking result included in these studies is the switch in relative metal binding affinities for the M8C, H4C, and H12C mutant proteins. The H12C mutant protein stacks more slowly than the wild-type protein in the Zn^{2+}- and Cu^{2+}-initiated reactions. However, the Co^{2+} reactions is 2-fold faster with H12C than with the wild-type protein. Clearly, the cysteine provides a good metal ligand, which may be further away from the metal binding site than the histidine side chain. An understanding of the differential effects of mutation for the different metal ions requires additional experiments.

The rate of stacking of the M8C mutant is nearly an order of magnitude faster than that of the wild-type GS, when Zn^{2+} is used to initiate the reaction. However, this mutant stacks approximately 4-fold more slowly than the wild type with Cu^{2+}. If the ratio of rate constants in the presence of Zn^{2+} vs Cu^{2+} is used as a measure of relative specificity for Zn^{2+}, then these data indicate that there is a 35-fold increase in the specificity of the M8C mutant for Zn^{2+} vs Cu^{2+}, compared to the wild type. The relative metal ion preference of the M8C protein is the reverse of the metal ion preference of the wild-type protein, which clearly stacks fastest with Cu^{2+}. It is not obvious, based on the model proposed here, why the M8C mutant protein does not bind Cu^{2+}. It is possible that the increase in the relative rate of stacking for the M8C mutant in the presence of Zn^{2+} and Co^{2+}, compared to the wild type, derives from the ability of the Cys side chain to form a bridging ligand to both metal ions. Thus,

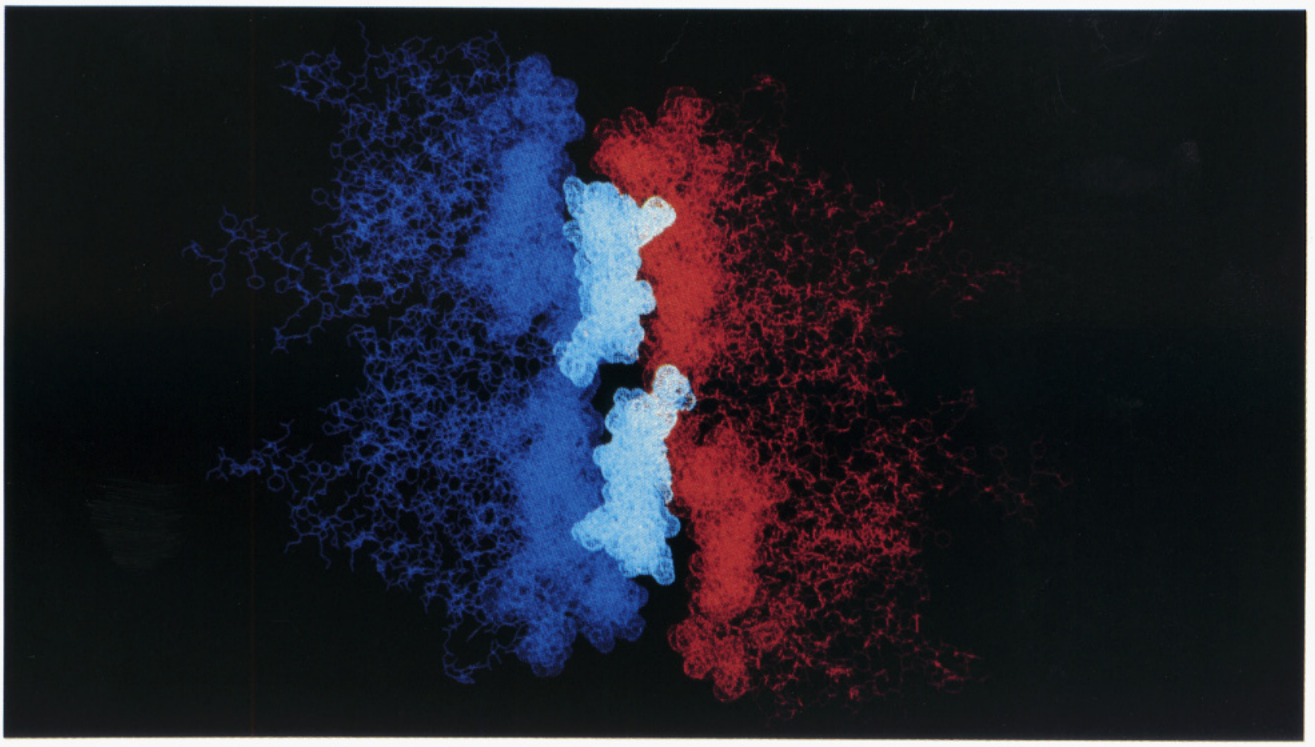

FIGURE 3: Van der Waals surface of the dodecamer interface. Two subunits of one dodecamer (red) and two subunits of a second dodecamer (blue) in the stacked complex are shown. The 6-fold axis runs horizontally within the page. The van der Waals surface of amino acids at the interface is shown, including the N-terminal helices (cyan). Between the interacting helices, large gaps are present which remain solvated.

with the M8C mutant, Zn^{2+} or Co^{2+} bound between dodecamers may be tetravalent with protein ligands. The sulfur atoms of Cys residues have been shown to provide bridging ligands in the binuclear site of the GAL4 transcription factor (Pan & Coleman, 1990). Interestingly, a binuclear purple copper site has recently been engineered in cytochrome *c* oxidase (Kelly et al., 1993). This site contains two histidines, two cysteines, and one methionine, and preliminary data indicate that one of the Cys residues provides a bridging ligand between two Co^{2+} ions. Although the detailed strucure of the ligands at the metal binding site requires further studies, the cysteine-containing mutants dramatically demonstrate the potential for engineering metal specificity by incorporation of new ligands.

In principle the Cys-containing mutants should provide direct spectroscopic evidence for Cys−metal ligation. This is based on the well-documented absorbance bands which are observed in the optical spectra of many Cu^{2+}-containing and Co^{2+}-containing proteins (Regan, 1993). However, due to their low molar extinction coefficients, absorbance bands for Cu^{2+}−Cys and Co^{2+}−Cys are observed typically at protein concentrations as high as 2−20 mg of protein/mL. In this concentration range, the Cys-containing GS mutants precipitate from solution, forming opaque samples, in the presence of Cu^{2+} or Co^{2+} [see Yanchunas et al. (1994)]. The spectra obtained from these samples are, therefore, difficult to interpret. Although we have observed weak absorbance bands in the range from 580 to 620 nm for samples of M8C and samples of H12C containing either Cu^{2+} or Co^{2+}, more sophisticated spectroscopic experiments will be required to determine unambiguously the wavelength maxima and molar extinction coefficients.

The size of GS complexes has prevented direct determination by mass spectrometry of the stoichiometry of the metal binding site responsible for the stacking reaction. However, atomic absorption and Zn^{2+} titration experiments have previously suggested a ratio of Zn^{2+}/GS subunit of 1, consistent with a binuclear site (Miller et al., 1974). In the context of this model, the results with the M8L mutant GS require comment. This mutant protein stacks more slowly than the wild type, but much more efficiently than either the H4A or H12L mutants. Apparently, the methionine ligand is not essential. For the binuclear site proposed here, it would be expected that substitution of Met-8 by a leucine would remove one ligand from both metals to produce two "weak" (His)-metal-(His) sites, whereas substitution of His-12 or His-4 with leucine or alanine, respectively, would remove two ligands from a single metal and leave one "strong" $(His)_2$-metal-(Met) site. The fact that the M8L mutant stacks, but the H4A and H12L mutants do not, suggests that two weak metal binding sites between helices more efficiently promote stacking than one strong metal binding site. Each metal binding site created at the boundary of N-terminal helices in adjacent dodecamers may be a low-affinity site, yet the stability of the dodecamer complex may be increased by the existence of multiple binding sties within the dodecamer interface, resulting from the symmetry of the dodecamer.

In addition to the metal ligands, other protein-derived features of the binding site are noteworthy. Interestingly, most of the N-terminal helix of each subunit is solvent inaccessible in the stacked complex. However, there is a striking solvent channel between the helices and the remainder of the subunits to which they are attached, which suggests that ions and water molecules have ready access to the binding site. It is well established that metal binding sites in proteins are often well insulated from solvent (Gregory et al., 1993). It has been observed that, in many naturally

occurring metal binding sites, polar residues, including the metal ligands, are found in close proximity to the metal, whereas hydrophobic residues form a second sphere around these polar residues. It has been suggested that the resulting "hydrophobic contrast" or "insulation" maximizes the strength of the ionic interactions between the protein and the metal ion (Regan, 1993; Gregory et al., 1993). The proposed metal binding site at the interface of GS dodecamers does not include a high degree of hydrophobic contrast. Although the N-terminal helices are amphipathic and hydrophobic residues lie on the side of the helices not involved in metal coordination, the metal binding sites are relatively solvent exposed.

Although the stoichiometry of metal binding and the precise geometry of metal ligands remain to be determined, the results presented here clearly implicate the N-terminal helix of GS as a region of focus in further understanding the mechanism of this supramolecular assembly reaction. These data provide a reasonable molecular mechanism for metal ion-initiated GS stacking without a conformational change of the individual subunits contained in GS.

ACKNOWLEDGMENT

The authors acknowledge Dr. Claudia Jochheim for helpful discussions and for help in preparation of the manuscript.

REFERENCES

Almassey, R. J., Janson, C. A., Hamlin, R., Xuong, N. H., & Eisenberg, D. (1986) *Nature 323*, 304−309.
Atkins, W. M. (1994) *Biochemistry 33*, 14965−14973.
Berg, J. M. (1993) *Curr. Opin. Struct. Biol. 3*, 585−588.
Betz, S. F., Raleigh, D. P., & DeGrado, W. F. (1993) *Curr. Opin. Struct. Biol. 3*, 601−610.
Chakrabarti, P. (1989) *Biochemistry 28*, 6081−6085.
Colombo, G., & Villafranca, J. J. (1987) *J. Biol. Chem. 264*, 10587−10591.
Fisher, M. T. (1993) *J. Biol. Chem. 268*, 13777−13779.
Frey, T. G., Eisenberg, D., & Eiserling, F. A. (1975) *Proc. Natl. Acad. Sci. U.S.A. 72*, 3402−3406.
Ghadiri, M. R., Soares, C., & Choi, C. (1992) *J. Am. Chem. Soc. 114*, 825−831.
Ginsburg, A., Yeh, J., Hennig, S. B., & Denton, M. D. (1970) *Biochemistry 9*, 633−649.
Glusker, J. R. (1991) *Adv. Protein Chem. 42*, 3−75.
Gregory, D. S., Martin, A. C. R., Cheetham, J. C., & Rees, A. R. (1993) *Protein Eng. 6*, 29−35.
Ho, S. N., Hunt, H. D., Horton, R. M., Pullen, J. K., & Pease, L. R. (1989) *Gene 77*, 51−59.
Karlin, K. D. (1993) *Science 261*, 701−708.
Lu, Y., LaCroix, L. B., Lowery, M. D., Solomon, E. I., Bender, C. J., Peisach, J., Roe, J. A., Gralla, E. B., & Valentine, J. S. (1993) *J. Am. Chem. Soc. 115*, 5907−5918.
Maurizi, M. R., Kasprzyk, P. G., & Ginsburg, A. (1986) *Biochemistry 25*, 141−151.
Meldrum, F. C., Wade, V. J., Nimmo, D. L., Heywood, B. R., & Mann, S. (1991) *Nature 349*, 684−685.
Miller, R. E., Shelton, E., & Stadtman, E. R. (1974) *Arch. Biochem. Biophys. 163*, 155−171.
Ozin, G. (1992) *Adv. Mater. 4*, 612−758.
Pan, T., & Coleman, J. E. (1990) *Proc. Natl. Acad. Sci. U.S.A. 87*, 2077−2081.
Regan, L. (1993) *Annu. Rev. Biophys. Biomol. Struct. 22*, 257−281.
Rosenfield, R. E., Parasarathy, R., & Dunitz, J. D. (1977) *J. Am. Chem. Soc. 99*, 4860−4862.
Sarkar, G., & Sommer, S. S. (1990) *Biotechniques 8*, 404−407.
Solomon, E. I., Baldwin, M. J., & Lowery, M. D. (1992) *Chem. Rev. 92*, 521−542.
Stadtman, E. R., Smyrniotis, P. Z., Davis, J. N., & Wiitenberg, M. E. (1979) *Anal. Biochem. 82*, 275−281.
Stayton, P. S., Olinger, J. M., Jiang, M., Bohn, P. W., & Sligar, S. G. (1992) *J. Am. Chem. Soc. 114*, 9298−9299.
Woolfold, C. A., Shapiro, B. M., & Stadtman, E. R. (1966) *Arch. Biochem. Biophys. 116*, 17−192.
Yamashita, M. M., Almassy, R. J., Janson, L. A., Lasek, D., & Eisenberg, D. (1989) *J. Biol. Chem. 264*, 17681−17689.
Yanchunas, J., Jr., Dabrowski, M. J., Schurke, P., & Atkins, W. M. (1994) *Biochemistry 33*, 14949−14956.